



## Immobilization of *Bacillus licheniformis* using Fe<sub>3</sub>O<sub>4</sub>@SiO<sub>2</sub> nanoparticles for the development of bacterial bioreactor

AYOUB NADI<sup>1,2,3</sup>, MAROUANE MELLOUL<sup>4</sup>, AICHA BOUKHRISS<sup>1</sup>, ELMOSTAFA EL FAHIME<sup>5</sup>,  
DAMIEN BOYER<sup>3</sup>, HASSAN HANNACHE<sup>6</sup> and SAID GMOUH<sup>2\*</sup>

<sup>1</sup>Laboratoire REMTEX, ESITH, route d'Eljadida, km 8, BP 7731 - Oulfa, Casablanca, Morocco.

<sup>2</sup>Laboratoire LIMAT, Université Hassan II Casablanca, BP: 9167 Casablanca, Morocco.

<sup>3</sup>Université Clermont Auvergne, CNRS, SIGMA Clermont, Institut de Chimie de Clermont-Ferrand, F-63000 Clermont-Ferrand, France.

<sup>4</sup>Laboratory of Physiology, Genetics and Ethnopharmacology – Faculty of Sciences Oujda – University Mohammed Premier Oujda, Oujda, Morocco.

<sup>5</sup>Assistance Units for Scientific and Technical Research, Allal Fassi/FAR corner, BP 8027, Hay Riad, 10000 Rabat, Morocco.

<sup>6</sup>Materials Science and Nanoengineering Department, Mohamed VI Polytechnic University, Lot 660–Hay Moulay Rachid, 43150 Benguerir, Morocco.

\*Corresponding author E-mail: said.gmouh@gmail.com

<http://dx.doi.org/10.13005/ojc/350249>

(Received: August 14, 2018; Accepted: March 29, 2019)

### ABSTRACT

In the biotechnology field, nanoparticles with a strong magnetic moment can bring attractive and novel potentialities. They are detectable, manipulable, stimuable by a magnetic field and they could be applied as nano-tracers for medical imaging and nano-vectors for transporting therapeutic agents to a target. For our part, we applied Fe<sub>3</sub>O<sub>4</sub> nanoparticles to immobilize bacteria of Moroccan strains in order to develop bacterial bioreactor. For this aim, we got through the synthesis and characterization of magnetite Fe<sub>3</sub>O<sub>4</sub> nanoparticles by co-precipitation in basic medium. The obtained nanoparticles were encapsulated in silica by sol-gel process. The results of this step allowed us to use Fe<sub>3</sub>O<sub>4</sub>@SiO<sub>2</sub> nanoparticles to immobilize *Bacillus licheniformis* by adsorption and separate it magnetically. The principle of this system gives us the opportunity to develop a bacterial bioreactor for industrial applications.

**Keywords:** Biotechnology, Iron oxide nanoparticles, Sol-gel, Cells immobilization, Magnetic separation.

### INTRODUCTION

The science of nanomaterials is one of the most important lines of research and development

in modern science. The use of nanoparticles has offered several advantages due to their size which generally does not exceed 100 nm and their unique physicochemical properties: Optical<sup>1</sup>, chemical<sup>2</sup>,



electrical<sup>3</sup>, mechanical<sup>4</sup> and magnetic<sup>4</sup>. The magnetic oxides nanoparticles are widely required in several applications: Electromechanical systems<sup>1,5</sup>, information storage<sup>5</sup>, catalysis<sup>6</sup> etc. This is due to their controllable dimension, chemical inertia and biocompatibility<sup>7</sup>. This makes them widely used in more specific applications, for example: magnetic assistance of drug delivery, treatment of cancer by hyperthermia, immobilization of enzymes and also as contrast agents in Magnetic Resonance Imaging(MRI)<sup>8</sup>.

Iron oxide nanoparticles form a very interesting system because of their susceptibility to change their magnetic behavior, inducing a transition between super-paramagnetic and ferrimagnetic behavior<sup>9</sup>. Indeed, iron oxide nanoparticles have a strong response to magnetization, which is no longer held after the end of exposure to the magnetic field. So, the separation or recovery of iron oxide nanoparticles could be assisted by a magnetic field produced by a permanent magnet<sup>10</sup>.

Recently,  $\text{Fe}_3\text{O}_4$  nanoparticles has gained enthusiastic attention from many researchers due to their unique properties in nano scale, such as a large surface area, high surface energy, low toxicity, biocompatibility, super-paramagnetic behavior, high absorption...etc<sup>11,12</sup>. Several methods have been proposed for the preparation of  $\text{Fe}_3\text{O}_4$  nanoparticles including hydrothermal process<sup>13</sup>, pyrolysis<sup>14</sup>, thermal decomposition of organometallic complexes in high-boiling point solvents<sup>12</sup> and the co-precipitation of Fe(III) and Fe(II) salts in the presence of an aqueous base<sup>15</sup>. However, co-precipitation has become the preferred method in preparing  $\text{Fe}_3\text{O}_4$  nanoparticles because of its many advantages, including short time reaction, the ability to use water as a solvent, cost effectiveness, simplicity, high productivity, as well as its low-temperature process. The presence of the iron cations under the two valence states  $\text{Fe}^{2+}$  and  $\text{Fe}^{3+}$  and the easy oxidation of the  $\text{Fe}^{2+}$  ions require careful control of the various synthesis steps. For this, working under inert atmosphere ( $\text{N}_2$  or Argon) is necessary to obtain a stoichiometric magnetite and to avoid the undesirable phases representing less interesting magnetic properties<sup>16,17</sup>. However, the limited mechanical properties, and the relative resistance of  $\text{Fe}_3\text{O}_4$  nanoparticles to the oxidation require a modification of their surface<sup>18</sup>. This could be done by different methods: adsorption, covalent bond, inclusion or encapsulation<sup>18</sup> and by the application of various organic polymers such as: polyethylene glycol<sup>19</sup>, polystyrene<sup>20</sup> and chitosan<sup>21</sup> etc.

Recently, the encapsulation of  $\text{Fe}_3\text{O}_4$  nanoparticles has been made towards mineral matrices such as  $\text{SiO}_2$ ,  $\text{ZrO}_2$ ,  $\text{TiO}_2$  representing improved mechanical properties<sup>21-23</sup>. The use of silica as a protective support presents numerous advantages: 1) non-toxicity and transparency<sup>24,2</sup> good *in-situ* dispersion of the nanoparticles by dipolar attraction which avoids their leaching<sup>25,3</sup> acceptable inertia and biocompatibility in different temperature and pH domains<sup>26,4</sup> the presence of the silanol group which increases their reactivity and facilitates the attachment to the target, thus ensuring a selective linkage with the functional organic molecules<sup>27</sup>. This increases the demand of iron oxide nanoparticles encapsulated in silica in biotechnology applications<sup>28</sup>, among others, the immobilization of the various microorganisms (enzymes, fungi, bacteria...etc<sup>29,30</sup>.

Our aim in this work was the immobilization of bacteria using  $\text{Fe}_3\text{O}_4 @ \text{SiO}_2$  nanoparticles to allow magnetic separation and recovery of the attached bacteria from their culture or reaction medium using a magnet. This new technology, known as "magnetic separation", guarantees an easy, quick, low cost and convenient method for eventual use in biotechnology and catalysis<sup>31</sup>. For this, magnetic iron oxide nanoparticles was synthesized by co-precipitation and then encapsulated in silica by a sol-gel process (Fig.1). Later, the immobilization of Moroccan thermophilic strains of *Bacillus licheniformis* by  $\text{Fe}_3\text{O}_4 @ \text{SiO}_2$  nanoparticles system was intended for the development of bacterial bioreactor.

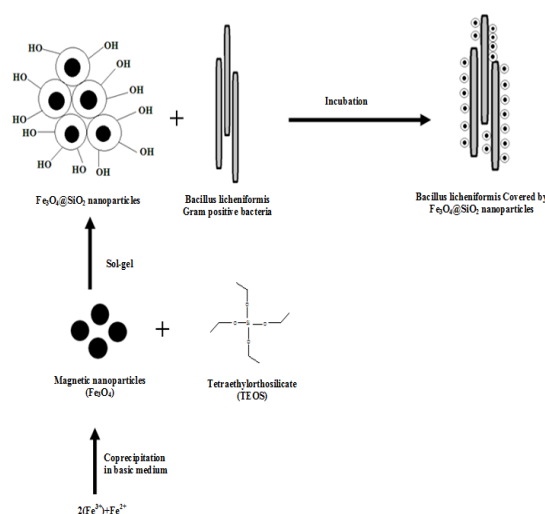


**Fig. 1. Illustration of *Bacillus licheniformis* immobilization process by magnetic nanoparticles encapsulated in silica**

## MATERIAL AND METHODS

### Chemicals

The following chemicals were used without further treatment and/or purification: Iron Chloride (III): FeCl<sub>3</sub>·6H<sub>2</sub>O (SOLVACHIM); Iron Chloride (II): FeCl<sub>2</sub>·6H<sub>2</sub>O (SIGMA-ALDRICH); Ammonium hydroxide: NH<sub>4</sub>OH, Solution 32% (SIGMA-ALDRICH); Tetraethylorthosilicate (TEOS): Si(OCH<sub>2</sub>CH<sub>3</sub>)<sub>4</sub> (SIGMA-ALDRICH).

## EXPERIMENTS

### Synthesis of Fe<sub>3</sub>O<sub>4</sub> nanoparticles

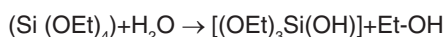
The deionized water (200 mL) was deoxygenated under N<sub>2</sub> for 1 h 30, and then 50 mL of NH<sub>4</sub>OH was added to the mixture and stirred at 1000 rpm. Amounts of 6.76 g of FeCl<sub>3</sub>·6H<sub>2</sub>O (2.5 mMol) and 4.97g of FeCl<sub>2</sub>·4H<sub>2</sub>O (1.25 mMol) were dissolved separately in 50 mL of the distilled water in order to prepare 0.5mol solutions. 10 mL of ferrous chloride and 20 mL of ferric chloride solutions were added to the solution of ammonium hydroxide. The mixture was stirred for 2.5 min at 100 rpm giving the formation of a black precipitate. The obtained product was washed 4 times with deionized water and the separation of the Fe<sub>3</sub>O<sub>4</sub> nanoparticles was done by a permanent magnet.

### Encapsulation of Fe<sub>3</sub>O<sub>4</sub> nanoparticles in silica

2 g of the Fe<sub>3</sub>O<sub>4</sub> nanoparticles was dispersed in millipore water and placed in a solution containing ethanol (80 mL) and water (40 mL). 3 mL of ammonium hydroxide NH<sub>4</sub>OH and 2 mL of tetraethylorthosilicate (TEOS) was added to this mixture and stirred for 24 hour. The obtained precipitate was separated and then washed 3 times with Millipore water and finally dried at 80°C in the oven.

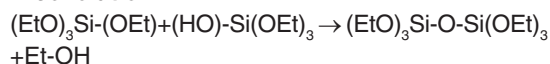
The encapsulation of the magnetic nanoparticles in the silica was done by sol-gel process using (TEOS) as silica precursor. The mechanism of this reaction follows the basic steps of sol-gel synthesis.

The hydrolysis in the presence of an inorganic base as catalyst allows the substitution of (O-Et) group by a hydroxyl (-OH) group according to the following reaction:

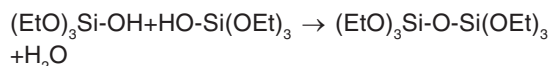


The condensation that results from the formation of the siloxane band following two parallel reactions:

### Alcoxolation



### Oxolation



### Immobilization of *Bacillus licheniformis*

In this study, we chose 3 Moroccan thermophilic strains of *Bacillus licheniformis* from 3 different regions of Morocco (Table 1), isolated and studied by Aanniz *et al.*,<sup>35</sup>. Bacteria were collected from a pure colony of *Bacillus licheniformis*, a *gram-positive* mesophilic bacterium. Its optimal growth temperature is around 50°C<sup>1</sup>. The colonies were inoculated into 5mL of TSB (Tryptone Soy Broth), and allowed to grow overnight. Then, 200 µL of the culture was transferred into 20 ml of TSB and incubated at 50°C for 24 hours. The bacteria were separated from their culture medium by centrifugation at a rate of 9000 rpm for 20 min. After removing the supernatant, 20 mg of the Fe<sub>3</sub>O<sub>4</sub>@SiO<sub>2</sub> nanoparticles was dispersed in 5 mL of sterilized distilled water containing the separated bacteria. In order to cover and immobilize the bacteria by the magnetic nanoparticles, the mixture was stirred at 150 rpm in an incubator at 50°C for 30 minutes. Then the precipitate was washed 3 times with sterilized distilled water to remove non-immobilized bacteria and the rest of the culture medium.

**Table 1: Provenances and backgrounds of *Bacillus licheniformis* strains**

Provenance	Medium
Oualidia	Salt water
Merzouga	Desert Sand
SidiMoussa	Salt water

### Identification of bacteria by the sequencing of the 16S rRNA gene

#### DNA extraction

Bacterial DNA was extracted from colonies of 3 samples from revitalized bacteria culture using the Sigma's GenElute Bacterial Genomic DNA Kit (Sigma-Aldrich, USA), according to manufacturer instructions. Briefly, 1.5 mL of bacterial broth culture

was pelleted at 12,000 to 16,000 ×g for 2 min; cells were resuspended in 200 μL of lysozyme (200 units/mL) and 20 μL of Proteinase K was added to the cell suspension. After incubation at 55°C for 30 min, 200 μL of lysis solution C was added to the suspension. The suspended cells were then incubated at 55°C for 10 min. DNA was purified using GenElute Miniprep Binding Columns (Sigma-Aldrich, USA). DNA was then eluted in sterile distilled water and stored at -20°C until use.

#### PCR and sequencing of the 16S rRNA gene

The 16S rRNA gene was amplified by PCR using primers fd1 (5'-AGA GTT TGA TCC TGG CTC AG-3') and Rp2 (5'-AAG GAG GTG ATC CAG CC-3'), as described by Weisburg *et al.*,<sup>39</sup>. PCR was carried out using 2.5 μL of 10 X buffer, 1.5mM of MgCl<sub>2</sub>, 0.2mM of each dNTPs, 0.4 μM of each primer, 1 U of Platinum Taq Polymerase (Invitrogen) and 100 ng of extracted DNA in a 25 μL reaction volume under the following conditions: 4 min at 96°C (initial denaturation), 35 cycles of 10s at 96°C (denaturation), 40s at 52°C (annealing), 2 min at 72°C (extension), and one final step of 4 min at 72°C (extension cycle) employing the PCR thermocycler "Veriti" (Applied Biosystems, Foster City, USA). The amplified fragments were electrophoresed on 1% agarose gel and detected using ethidium bromide along with molecular weight markers (1kb). The PCR products were purified using EXOSAP-IT (Affymetrix, USA) and sequenced on an ABI 3130 XI automated sequencer (Applied Biosystems, Foster City) using BigDye Terminator version 3.1 Kits with the primer. The analysis of electrophoregram was done using the sequencing Analysis Software version 5.3.1 (Applied Biosystems, Foster City, USA).

The consensus sequences were edited and compared with published sequences available in GenBank, using BLAST tool of the NCBI. The criterion used to identify an isolate to the genus or species level was suggested by several research works: 97 and 99% identity in 16S rRNA gene sequence to identify an organism to the genus and the species level, respectively.

#### Analytical methods

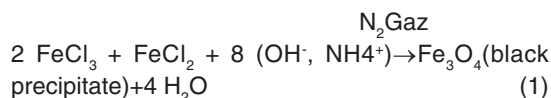
The crystalline phases of nanoparticles were identified using PANalytical X'pert diffractometer with a CuKα radiation (λ = 1.5406 Å). The characteristic vibration bands of nanoparticles were studied using

an infrared microscope (BRUCKER HYPERION 1000) in Attenuated Total Reflectance (ATR) configuration. The microstructure, morphology and EDX analysis of magnetic nanoparticles as well as the immobilized bacteria were analyzed by transmission electron microscope (TECNAI G2/ FEI). The surface areas of the bacteria immobilized by iron oxide nanoparticles were observed using an environmental scanning electron microscope (ESEM FEI QUANTA 200). The optical density was measured in order to calculate the efficiency of the immobilization of the bacteria by means of a spectrophotometer (Themospectronic Helios Gamma).

## RESULTS AND DISCUSSION

#### Synthesis of Fe<sub>3</sub>O<sub>4</sub> nanoparticles

For the synthesis of the magnetite nanoparticles, we have opted for a direct co-precipitation method in alkaline medium. It consists of mixing Fe<sup>3+</sup> and Fe<sup>2+</sup> sources with a molar ratio of 2/1 under an inert gas stream to remove oxygen and avoid oxidation. When the environment is not maintained inert, the oxidation of the Fe<sup>2+</sup> ions is carried out automatically giving the formation of a brown FeOH<sub>3</sub> precipitate, which affects the physicochemical properties of the magnetic nanoparticles. In order to avoid this problem, it is essential to work in an inert environment that is under an inert gas stream. In our case we used nitrogen as a carrier gas. The pH of the solution is increased until it exceeds 11 by adding a strong base. This causes a color change of the solution from orange to brown and then to black marking the end of the reaction (Fig. 2). The choice of chlorides as iron salts for the synthesis of Fe<sub>3</sub>O<sub>4</sub> is based on their good stability and solubility unlike sulphates and nitrates, which are easily oxidized and gives products that are difficult to remove (equation 1)<sup>32</sup>.



In order to assess the morphology, size, chemical composition and dispersion of the magnetic nanoparticles, TEM-EDX analysis have been performed and reported in Fig. 3. As showed in Fig.3-a, nanoparticles exhibit a quite spherical morphology and their average size found to be around 15 nm. However, the agglomeration of Fe<sub>3</sub>O<sub>4</sub> nanoparticles is observed. This is may be due to

their large surface-to-volume ratio and high surface energy<sup>33</sup>. The chemical elemental analysis EDX (Fig.3-b) evidenced the presence of iron oxide, and the atomic percentage indicated the presence of  $\text{Fe}_3\text{O}_4$  phase.

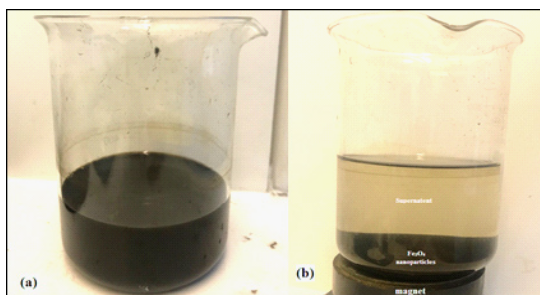


**Fig. 2.** Magnetic separation of iron oxide nanoparticles in solution: (a)  $\text{Fe}_3\text{O}_4$  nanoparticles in suspension; (b) precipitation of  $\text{Fe}_3\text{O}_4$  nanoparticles after the application of a magnetic field

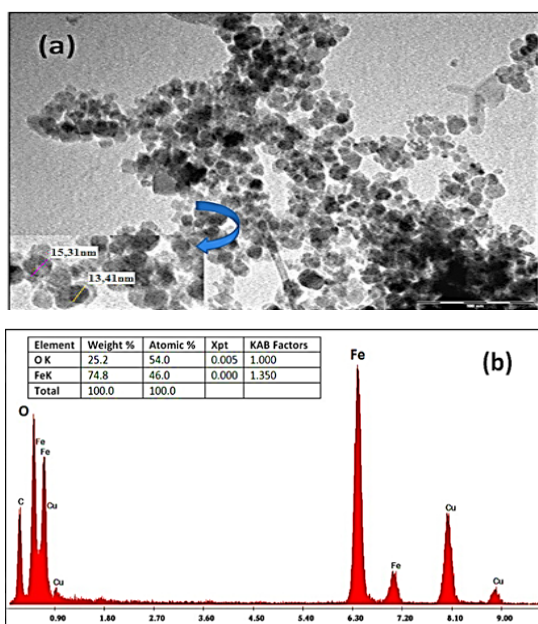


**Fig. 3.** (a) TEM images (b) EDX spectrum of iron oxide nanoparticles

The Fourier Transform Infrared (FTIR) spectrum of  $\text{Fe}_3\text{O}_4$  nanoparticles plotted in Fig.4 shows the appearance of the bands at around 1620 and 3437  $\text{cm}^{-1}$  corresponding to the H-O-H stretching modes ( $\nu\text{OH}$ ) and bending vibration ( $\delta\text{OH}$ ) of the free or adsorbed water, respectively. The band at 567  $\text{cm}^{-1}$  is related to the Fe-O bending vibration characteristic of the iron oxide.

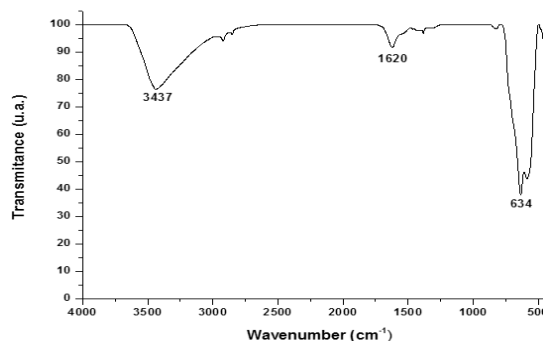


**Fig. 4.** FTIR spectrum of iron oxide nanoparticles

In the XRD pattern of iron oxide nanoparticles (Fig. 5) diffraction peaks with  $2\theta$  at 18.31°; 30.47°; 35.81°; 39.05°; 43.49°; 54.05°; 57.59° and 63.11° were observed, indicative of the crystalline structure of  $\text{Fe}_3\text{O}_4$ . According to the ICSD data base model No. 029129, the  $\text{Fe}_3\text{O}_4$  nanoparticles have a cubic spinel structure with lattice parameters of  $a = b = c = 8.31 \text{ \AA}$ .

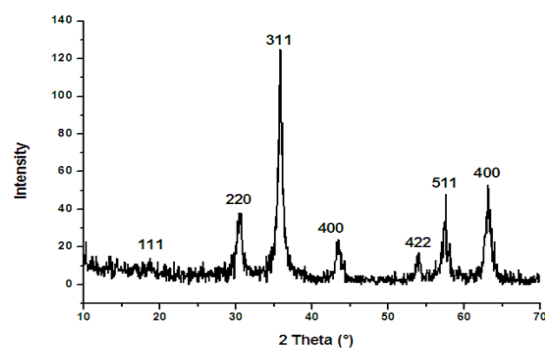


**Fig. 5.** XRD pattern of iron oxide nanoparticles

### Synthesis of $\text{Fe}_3\text{O}_4@SiO_2$ nanoparticles

The encapsulation of magnetic nanoparticles in silica was evidenced by TEM-EDX analysis (Fig.6). TEM observation shows the appearance of transparent layer of silica covering the magnetic nanoparticles (Fig.6-a), which is confirmed by the appearance of Si peaks in EDX analysis (Fig.6-c). The increase in the size of the nanoparticles is due to the formation of  $\text{SiO}_2$  layer of about 10 nm at their surface while maintaining the spherical morphology (Figure 6-b).

The X-ray diffraction pattern of the  $\text{Fe}_3\text{O}_4@SiO_2$  (Fig.7) shows the appearance of most of the peaks corresponding to the magnetic nanoparticles. The disappearance of some peaks and the weakness of the others are explained by the presence of the organic silica having an amorphous

nature, which covers the entire surface of the magnetic nanoparticles and forms a screen preventing X-ray diffraction on the crystal phase of the sample.

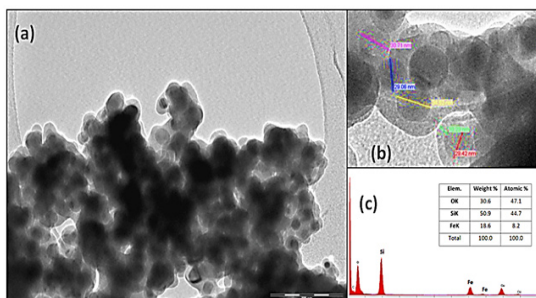


Fig. 6. (a), (b) TEM images of  $\text{Fe}_3\text{O}_4@SiO_2$  nanoparticles; (c) EDX analysis of  $\text{Fe}_3\text{O}_4@SiO_2$  nanoparticles.

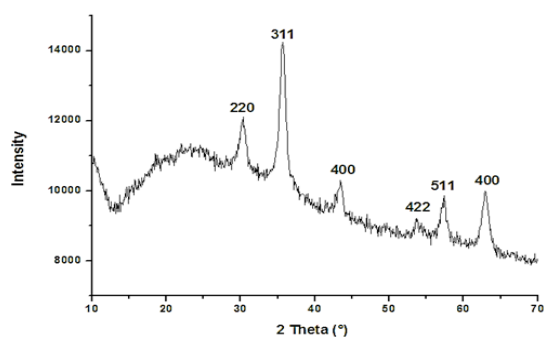


Fig. 7. XRD patterns of iron oxide nanoparticles encapsulated in silica  $\text{Fe}_3\text{O}_4@SiO_2$

The Fourier transform infrared (FTIR) spectra of  $\text{Fe}_3\text{O}_4@SiO_2$  illustrated in Fig. 8, shows the presence of a broad high-intensity band at  $1101\text{ cm}^{-1}$  corresponding to the motion of oxygen in Si-O-Si antisymmetric stretch, due to the asymmetric stretching bonds of Si-O-Si in  $SiO_2$ . The band at  $802\text{ cm}^{-1}$  is assigned to the Si-O-Si symmetric stretch, while the band at  $470\text{ cm}^{-1}$  corresponds to the Si-O-Si or O-Si-O bending modes. The band at  $943\text{ cm}^{-1}$  is assigned to the Si-O symmetric stretch. The band at  $617\text{ cm}^{-1}$  indicates the presence of Si-O-Fe and confirms the formation of a bond between the metallic nanoparticles and the organic silica.

#### Immobilization of *Bacillus licheniformis* $\text{Fe}_3\text{O}_4@SiO_2$ nanoparticles

The immobilization of *Bacillus Licheniformis* was carried out by magnetic nanoparticles encapsulated in the silica at  $\text{pH}=7$ . Then the percentage of the efficiency of this immobilization was calculated according to the following equation (2):

$$\text{Immobilization efficiency (\%)} = \frac{OD_{600\text{before}} - OD_{600\text{after}}}{OD_{600\text{before}}} \times 100 \quad (2)$$

\* $OD_{600}$ : Optical density measured by the spectrophotometer at a wavelength of  $600\text{ nm}$ .

The immobilization efficiencies of  $\text{Fe}_3\text{O}_4@SiO_2$  nanoparticles for *Gram-positive* bacteria were up to 60 % (Fig. 9) for the strains. The possible explanation is that the major components of the cell wall of *Gram-positive* bacteria are peptidoglycan and teichoic acids<sup>36</sup>. Teichoic acid is a long phosphodiester polymer also containing phosphate groups in addition to alanine and N-acetylglucosamine groups<sup>37</sup>. The alanine groups have been reported to be responsible for the attachment of lipoteichoic acid onto  $SiO_2$ . The alanine groups are positively charged ( $-NH_3^+$ ) while  $SiO_2$  is negatively charged<sup>38</sup>. Also, it has been reported that  $SiO_2$  particles carry negative charges at  $\text{pH}=7$ <sup>30</sup>, suggesting that the immobilization mechanism includes not only electrostatic attraction, but also other intermolecular interactions such as covalent and hydrogen bonding.

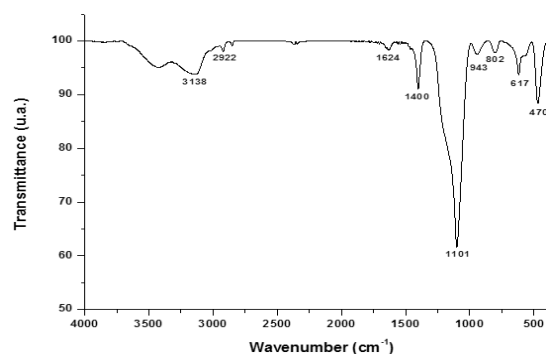


Fig. 8. FTIR spectra of iron oxide nanoparticles encapsulated in silica

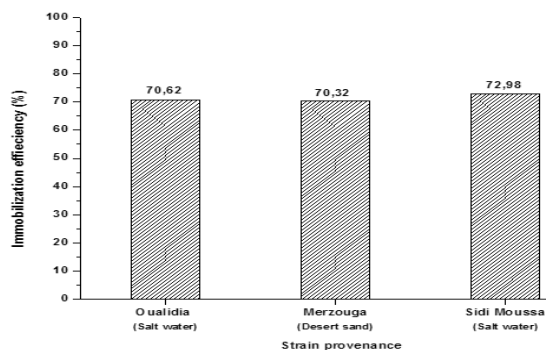


Fig. 9. Immobilization efficiency of *Bacillus licheniformis* strains from different provenances

In the SEM images (Fig.10), we noticed the presence of the magnetic nanoparticles encapsulated in the silica on the surface of the bacteria. Despite its size (around 500µm), *Bacillus licheniformis* was easily separated from its culture medium by the magnetic method and in less than 2 minute.

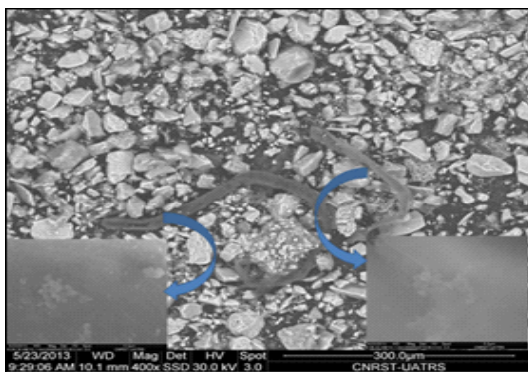


Fig. 10. SEM images of *Bacillus licheniformis* immobilized by  $\text{Fe}_3\text{O}_4@\text{SiO}_2$  nanoparticles

The results of the electron microscopy remain defective to confirm the biocompatibility of the  $\text{Fe}_3\text{O}_4@\text{SiO}_2$  nanoparticles in contact with the bacteria, because they do not signal the viability of the bacteria after the immobilization by the  $\text{Fe}_3\text{O}_4@\text{SiO}_2$  nanoparticles. We also have to confirm the absence of contamination during the steps following immobilization. For these reasons, we carried out a revitalization test and then the identification of the bacteria by the 16S rRNA gene sequencing.

#### Revitalization and identification of grafted bacteria

##### A) Revitalization test

To ensure the survival of our bacteria, we carried out a biological revitalization test. After drying the magnetic nanoparticles encapsulated in the silica, we inoculated a small amount in a sterile TSB medium (culture medium). The mixture was incubated at 55°C for 24 h, the appearance of a turbidity (Fig. 11) shows that the strains have grown and are viable.

##### B) Identification of bacteria by 16S rRNA gene sequencing

The 16S ribosomal RNA gene is widely present in all bacterial species, it codes for RNA component of the bacterial ribosome. The sequencing of the 16S rRNA gene is considered the

new gold standard for the specification of bacteria<sup>40</sup>. It is used as a tool for the identification of bacteria at the species level, and it assists by differentiating between closely related bacterial species<sup>41</sup>. In this study, we used the 16S rRNA sequencing technology to identify the bacteria *Bacillus licheniformis* used in the process of immobilization by  $\text{Fe}_3\text{O}_4@\text{SiO}_2$  nanoparticles. PCR of the 16SrRNA of the three bacteria showed unique bands at 1500pb (Fig.12), which represent a specific amplification of the 16S full gene. The purified PCR product of the sample 2 was then used for sequencing with the primer fD1. The sequence obtained (560 bases) was aligned with available sequences in GenBank database. The alignment showed an exact match with the bacteria *Bacillus licheniformis* (100% identity) used in this study under the Accession number KF879189. These results indicated that even after several processes (Immobilization, washing, etc.), we did not have any contamination or fixation of other contaminant bacteria.

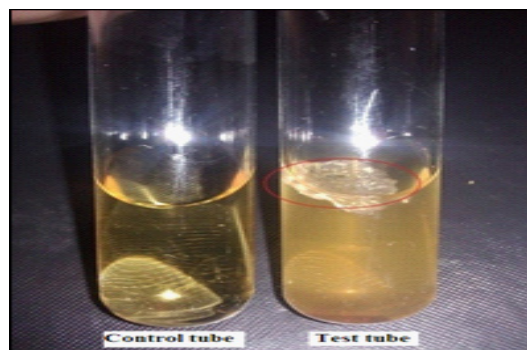


Fig. 11. Revitalization test of bacteria immobilized by  $\text{Fe}_3\text{O}_4@\text{SiO}_2$  nanoparticles

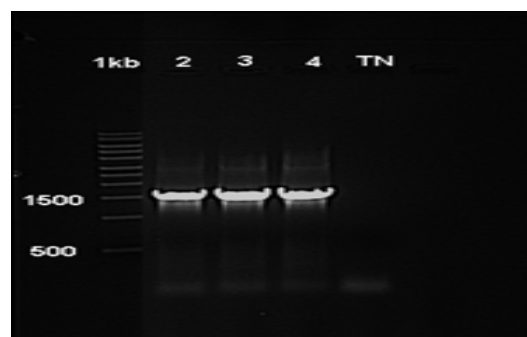


Fig. 12. PCR amplification of 16srRNA full gene using DNA extracted from overnight cultured bacteria controlled by Electrophoresis. 1kb is molecular weight, sample 2: Oualdia, sample 3: Merzouga, sample 3: Sidi Moussa and TN is negative control

## CONCLUSION

In this paper, we succeeded in synthesizing magnetite nanoparticles by co-precipitation of ferrous and ferric chlorides, then we encapsulated the iron oxide nanoparticles in the silica by hydrolysis and then TEOS condensation in a sol-gel process. The obtained nanoparticles of approximately 50 nm were realized while maintaining the morphology and the magnetic properties of iron oxide nanoparticles. The success of this step was confirmed by the formation of the Fe-O-Si band on the surface of the Fe<sub>3</sub>O<sub>4</sub> nanoparticles. Fe<sub>3</sub>O<sub>4</sub>@SiO<sub>2</sub> nanoparticles were intended to immobilize *Bacillus licheniformis*. After achieving the grafting and the magnetic separation of bacteria, the biocompatibility and

non-toxicity of Fe<sub>3</sub>O<sub>4</sub>@SiO<sub>2</sub> nanoparticles to the *Bacillus licheniformis* and was proven by the revitalization test. The satisfactory results of this work open new horizons towards the development of a bacterial bioreactor for industrial applications. In our perspectives, we are thinking about using Fe<sub>3</sub>O<sub>4</sub>@SiO<sub>2</sub> nanoparticles to immobilize bacterial cells for the treatment of polluted industrial effluents and enjoy the magnetic separation of cells to concept a recyclable bacterial bioreactor.

## ACKNOWLEDGEMENT

The authors gratefully acknowledge Campus France for the financial support through PHC Toubkal project N°32506VM.

## REFERENCES

- Zhang, Y. X.; Wang, Y. H. *RSC Adv.*, **2017**, *7*, 45129-45144.
- Hauser, A. K.; Mathias, R.; Anderson, K. W.; Hilt, J. Z. *Mat. chem. phy.*, **2015**, *160*, 177-186.
- Hong, C. S.; Park, H. H.; Moon, J.; Park, H. H. *T. S. Films.*, **2006**, *515*, 957-960.
- Ali, A.; Hira Zafar, M. Z.; ul Haq, I.; Phull, A. R.; Ali, J. S.; Hussain, A. *Nanotechnol. sci. appl.*, **2016**, *9*, 49.
- Ekinci, K. *Small.*, **2005**, *1*, 786-797.
- Neamtu, M.; Nadejde, C.; Hodoroaba, V. D.; Schneider, R. J.; Verestiuc, L.; Panne, U. *Sci. rep.*, **2018**, *8*, 6278.
- Mirzaei, H.; Darroudi, M. *Ceram. Int.*, **2017**, *43*, 907-914.
- Mehta, R. *Mat. Sci. Eng. C.*, **2017**, *79*, 901-916.
- Shi, D.; Sadat, M. E.; Dunn, A. W.; Mast, D. B. *Nanoscale.*, **2015**, *7*, 8209-8232.
- Xu, H.; Aguilar, Z. P.; Yang, L.; Kuang, M.; Duan, H.; Xiong, Y.; Wang, A. *Biomater.*, **2011**, *32*, 9758-9765.
- Nochehdehi, A. R.; Thomas, S.; Sadri, M.; Afghahi, S. S. S.; Hadavi, S. M. *J. Nanomed. Nanotechnol.*, **2017**, *8*, 1000423.
- Reddy, L. H.; Arias, J. L.; Nicolas, J.; *Couvreur, P. Chem. Rev.*, **2012**, *112*, 5818-5878.
- Cai, H.; An, X.; Cui, J.; Li, J.; Wen, S.; Li, K.; Shi, X. *ACS Appl. Mat. Inter.*, **2013**, *5*, 1722-1731.
- Wei, H.; Bruns, O. T.; Kaul, M. G.; Hansen, E. C.; Barch, M.; Wisniewska, A.; Cordero, J. M. *Proceed. Nat. Aca. Sci.*, **2017**, *114*, 2325-2330.
- Kandpal, N. D.; Sah, N.; Loshali, R.; Joshi, R.; Prasad, J. *J. Sci. Ind. Res.*, **2014**, *73*, 87-90.
- Manukyan, K. V.; Yeghishyan, A. V.; Shuck, C. E.; Moskovskikh, D. O.; Rouvimov, S.; Wolf, E. E.; Mukasyan, A. S. *J. Micro. Meso. Mat.*, **2018**, *257*, 175-184.
- Lee, D. K.; Song, Y.; Kim, J.; Park, E. Y.; Lee, J. *J. Col. Inter. Sci.*, **2017**, *499*, 54-61.
- Keyhanian, F.; Shariati, S.; Faraji, M.; Hesabi, M. *Arab. J. Chem.*, **2016**, *9*, 348-354.
- Xu, K.; Wang, Y.; Zhang, H.; Yang, Q.; Wei, X.; Xu, P.; Zhou, Y. *Microchim. Acta.*, **2017**, *184*, 4133-4140.
- Hen, Y.; Wang, Y.; Zhang, H. B.; Li, X.; Gui, C. X.; Yu, Z. Z. *Carbon.*, **2015**, *82*, 67-76.
- Ding, Y.; Shen, S. Z.; Sun, H.; Sun, K.; Liu, F.; Qi, Y.; Yan, J. *Mat. Sci. Eng. C.*, **2015**, *48*, 487-498.
- Noormohamadi, A.; Homayoonfal, M.; Mehrnia, M. R.; Davar, F. *Ceram. Int.*, **2017**, *43*, 17174-17185.
- Liu, F. M.; Zhang, Y.; Yin, W.; Hou, C. J.; Huo, D. Q.; He, B.; Fa, H. B. *Sens. Act. B Chem.*, **2017**, *242*, 889-896.
- Liu, J. N.; Bu, W. B.; Shi, J. L. *Acc. Chem. Res.*, **2015**, *48*, 1797-1805.
- Kaleji, B.; Mousaei, M.; Halakouie, H.; Ahmadi, A. *J. Nano Struct.*, **2015**, *5*, 219-225.
- Catauro, M.; Papale, F.; Roviello, G.; Ferone, C.; Bollino, F.; Trifuoggi, M.; Aurilio, C. *J. Biomed. Mat. Res. A.*, **2014**, *102*, 3087-3092.
- Lovino, G.; Agnello, S.; Gelardi, F. M.; Boscaino, R. D. *J. Phys. Chem. C.*, **2014**, *118*, 18044-18050.

28. Zelepukin, I. V.; Shipunova, V. O.; Mirkasymov, A. B.; Nikitin, P. I.; Nikitin, M. P.; Deyev, S. M. *Ac. Nat.*, **2017**, *9*, 34.
29. Tao, Q. L.; Li, Y.; Shi, Y.; Liu, R. J.; Zhang, Y. W.; Guo, J. *J. nanosci. nanotech.*, **2016**, *16*, 6055-6060.
30. Reddy, P. M.; Chang, K. C.; Liu, Z. J.; Chen, C. T.; Ho, Y. P. *J. biomed. nanotech.*, **2014**, *10*, 1429-1439.
31. Wang, C.; Zhang, K.; Zhou, Z.; Li, Q.; Shao, L.; Hao, R. Z.; Wang, S. *Int. J. Nanomed.*, **2017**, *12*, 3077.
32. Monteagudo, J. M.; Durán, A.; González, R.; Expósito, A. *J. Ap. Cat. B.*, **2015**, *176*, 120-129.
33. Yeap, S. P.; Lim, J.; Ooi, B. S.; Ahmad, A. L. *J. Nanopart. Res.*, **2017**, *19*, 368.
34. Hong, S. J.; Park, G. S.; Jung, B. K.; Khan, A. R.; Park, Y. J.; Lee, C. H.; Shin, J. H. *J. Appl. Biol. Chem.*, **2015**, *58*, 247-251.
35. Aanniz, T.; Ouadghiri, M.; Melloul, M.; Swings, J.; Elfahime, E.; Ibjijjen, J.; Amar, M. *Braz. J. Microbiol.*, **2015**, *46*, 443-453.
36. Brown, L.; Wolf, J. M.; Prados-Rosales, R.; Casadevall, A. *Nat. Rev. Microbio.*, **2015**, *13*, 620.
37. Schade, J.; Weidenmaier, C. *FEBS Lett.*, **2016**, *590*, 3758-3771.
38. Brown, M. A.; Abbas, Z.; Kleibert, A.; Green, R. G.; Goel, A.; May, S.; Squires, T. M. *Phys. Rev. X.*, **2016**, *6*, 011007.
39. Albertsen, M.; Karst, S. M.; Ziegler, A. S.; Kirkegaard, R. H.; Nielsen, J. *P. One.*, **2015**, *10*, e0132783.
40. Yoon, S. H.; Ha, S. M.; Kwon, S.; Lim, J.; Kim, Y.; Seo, H.; Chun, J. *Int. J. Syst. Evol. Microbiol.*, **2017**, *67*, 1613-1617.
41. Ruppitsch, W.; Pietzka, A.; Prior, K.; Bletz, S.; Fernandez, H. L.; Allerberger, F.; Mellmann, A. *J. Clin. Microbiol.*, **2015**, *15*, 01193.